

## (001) textured PbTiO<sub>3</sub> thin films grown on redoping *n*-Si by metalorganic chemical vapor deposition under reduced pressure

L. Sun<sup>1,\*</sup>, Y.-F. Chen<sup>1</sup>, T. Yu<sup>1</sup>, N.-B. Ming<sup>1</sup>, D.-S. Ding<sup>2</sup>, Z.-H. Lu<sup>2</sup>

<sup>1</sup>National Laboratory of Solid State Microstructures, Nanjing University, Nanjing 210093, P. R. China

<sup>2</sup>Laboratory of Molecular and Bio-molecular Electronics, South-East University, Nanjing 210013, P.R. China

Received: 23 February 1996/Accepted 21 May 1996

**Abstract.** (001) textured PbTiO<sub>3</sub> thin films have been deposited on (001) redoping *n*-Si substrates by metalorganic chemical vapor deposition (MOCVD) under reduced pressure, and the film ferroelectricity has been measured using the substrate as bottom electrode directly. Besides this investigation, a set of analysis including AFM surface morphology, SEM cross section morphology, electron-probe element analysis, XRD  $\theta$ - $2\theta$  scan and high temperature X-ray diffraction have been carried out to study the microstructure and phase transition process of the PbTiO<sub>3</sub> thin film.

**PACS:** 68.55JR; 81.15Gh

Among the various ferroelectric materials, PbTiO<sub>3</sub>, with large spontaneous polarization, small dielectric constant, small coercive field, high Curie temperature (490 °C) [1] and good chemical stability, has been utilized for non-volatile random access memories (FRAM), infrared (IR) detectors, surface acoustic wave (SAW) transducers, electro-optic devices and high-frequency transducers, etc. [2, 3, 4]. The use of MOCVD technique to deposit PbTiO<sub>3</sub> ferroelectric thin film began in 1988 [5], and epitaxial films have been deposited on (001) MgO [6, 7], (001) KTaO<sub>3</sub> [8], (012) LaAlO<sub>3</sub> [9] and (001) SrTiO<sub>3</sub> [10–14] single crystal substrates. However, to meet the device requirements for applications, the ferroelectric films should be deposited on the electrode-precoated substrates, and, more attractively, become integrated in silicon semiconductor technology. But the traditional Pt or Ti metallic electrodes react with Si substrate and the formed silicide will prevent the growth of ferroelectrics [15]. Recently, perovskite superconductors such as YBa<sub>2</sub>Cu<sub>3</sub>O<sub>7-x</sub> (YBCO), Bi<sub>2</sub>Sr<sub>2</sub>Cu<sub>2</sub>O<sub>8-x</sub> (BSCCO) and the novel perovskite-type oxides such as La<sub>0.5</sub>Sr<sub>0.5</sub>CoO<sub>3</sub> (LSCO) and LaNiO<sub>3</sub> have been explored as electrodes with success of improving the

fatigue property of the ferroelectric thin films [16–18] on lattice matched substrates, but high quality films on Si substrates are still hard to obtain. In this letter, we report the use of redoping Si wafer as substrate for the growth of PbTiO<sub>3</sub> thin film, and the ferroelectricity of the film was measured without pre-grown a layer of conducting materials. The MOCVD PbTiO<sub>3</sub> thin film is highly *c*-axis oriented and has a smooth surface which is very important for the fabrication of multilayer heterostructures.

The Si substrates used in the experiment are redoping (001) *n*-Si single crystal wafers with a resistivity of about  $5 \times 10^{-4} \Omega \cdot \text{cm}$ . Before the deposition, the Si wafers were cleaned with a standard semiconductor procedure, and right after the chemical rinse process, the substrate was moved into the reaction chamber.

PbTiO<sub>3</sub> thin films were prepared in a horizontal cool-wall MOCVD apparatus which has been described in detail elsewhere [13]. Purified titanium-iso-propoxide (TIP) and tetra-ethyl-lead (TEL) were used as the metalorganic precursors and their temperature was maintained at 65 °C and 35 °C in the oil baths during the grow-process. By adjusting the substrate temperature, total reaction pressure, partial pressure of O<sub>2</sub>, and flow rates of the MO vapors and N<sub>2</sub> (carrier gas), optimum growth conditions were established experimentally as listed in Table 1.

As-deposited films were specular and adhere well to the Si substrates. A Hitachi X-650 scanning electron microscope was used to observe the cross-section morphology of the film. The film was dense and has a smooth surface. An abrupt interface between the film and substrate can be seen in Fig. 1.

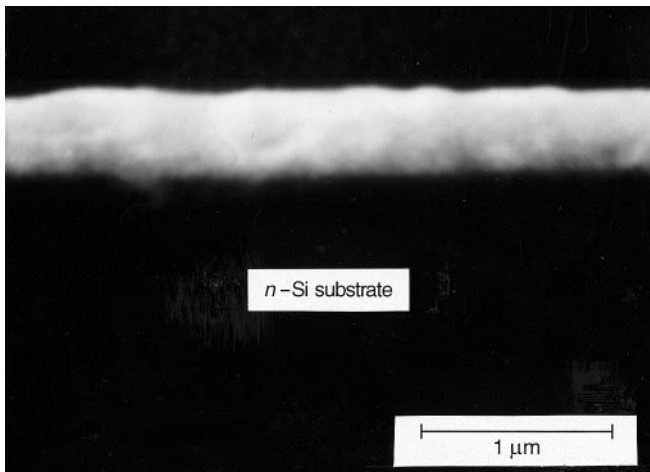
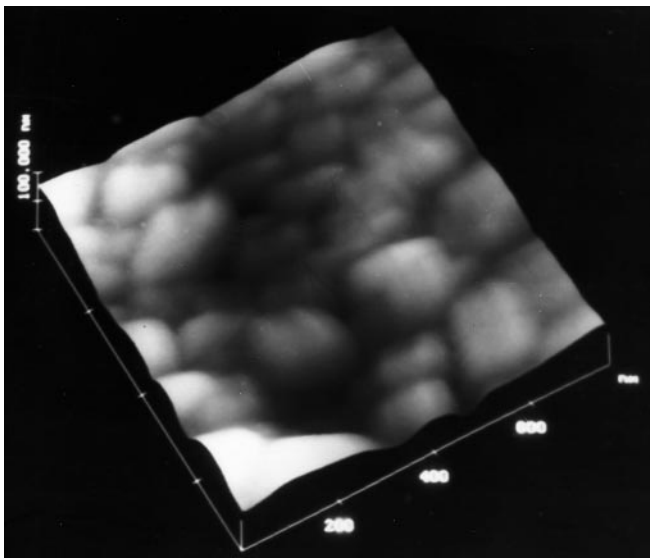
Further investigation of the film microstructure was carried out on a Nanoscope III atomic force microscopy (AFM). Figure 2 displays a typical AFM surface image of the as-deposited PbTiO<sub>3</sub> film; no obvious crack can be discerned on the film surface and the average grain size is determined to be 120 nm.

The film thickness was measured by a surface profilometer at the film edge which was made by selective deposition through a cover-glass mask. The measured thickness of 5000 Å was consistent with SEM observation, and the deposition rate was determined to be 33 Å/min.

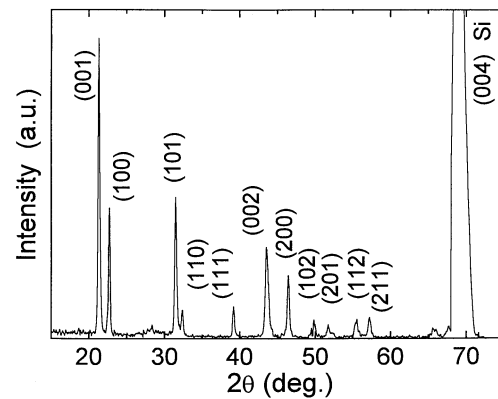
\*(Fax: + 86-25/3300-535, E-mail: yfchen@nju.edu.cn)

**Table 1.** Typical deposition conditions for MOCVD PbTiO<sub>3</sub>

Substrate	(001) redoping n-Si
Substrate temperature	650 °C
Reactor pressure	12.0 Torr
Carrier gas	N <sub>2</sub>
T <sub>TIP</sub>	65 °C
T <sub>TEL</sub>	35 °C
TEL carrier flow rate	80 sccm
TIP carrier flow rate	50 sccm
O <sub>2</sub> flow rate	100 sccm

**Fig. 1.** The cross-section scanning electron micrograph of the PbTiO<sub>3</sub> thin film on (001) Si**Fig. 2.** AFM surface morphology of the as grown PbTiO<sub>3</sub> thin film on Si substrate

To identify the phases in the as-deposited PbTiO<sub>3</sub> thin film, XRD  $\theta$ - $2\theta$  scan measurement was carried out on a Rigaku D/MAX-RA powder diffractometer with nickel-filtered Cu K $\alpha$  radiation. As shown in Fig. 3, no peaks

**Fig. 3.** The XRD 0–20 XRD scan pattern of PbTiO<sub>3</sub> thin films deposited on the Si substrate

other than the perovskite PbTiO<sub>3</sub> and the (004) reflection of Si substrate have been detected, the reflections of PbTiO<sub>3</sub> show a typical polycrystalline pattern. In the PbTiO<sub>3</sub> powder diffraction pattern, the intensity of the (100) plane is twice bigger than that of the (001) plane, so the c-axis orientation ratio  $\alpha$  can be defined as follows:

$$\alpha = I(001)/\{I(001) + I(100)/2\}$$

where  $I(100)$  and  $I(001)$  represent the intensity of (001) and (100) reflections respectively. The  $\alpha$  of this polycrystalline film is calculated to be 0.83, indicating a strong (001) texture, and because this is the direction of the spontaneous polarization of PbTiO<sub>3</sub>, it causes the remnant polarization of the film perpendicular to the plane of the substrate. Use the lattice constant of Si as a calibration, the c-axis length of PbTiO<sub>3</sub> was determined to be  $4.128 \pm 0.002$  Å, which is much smaller than in the bulk single crystal (4.150 Å), indicating the evidence of a size effect when the grain size is down to several hundred nanometers.

Using a Joel JXA-8800M electron probe, the composition of the thin film was examined. Only Pb, Ti, O and Si could be detected using different spectro-crystals. By analyzing four random plots on the film surface, the average atomic ratio of the three elements was: 1(Pb):1.08(Ti):3.21(O), which showed a small deficiency of Pb, and a thin layer of SiO<sub>2</sub> formed in the deposition process, maybe the cause of the stoichiometric deviation of O. Figure 4 is the Pb and Ti surface distribution photograph of the thin film; the gray scale indicates the relative content of the element, and in the examined area of  $50 \mu\text{m} \times 50 \mu\text{m}$  the two elements distribute uniformly.

The phase transition process of the polycrystalline PbTiO<sub>3</sub> thin film was investigated by high temperature X-ray diffraction. The sample was placed in the center of a triangle-column coiled with pt resistance thread in order to create a uniform temperature field. A thermocouple was fixed directly on the back of the sample for temperature measurement. The rate of heating and cooling was kept at 4 °C/min. Figure 5 shows the diffraction profile near the (002) and (200) peaks of PbTiO<sub>3</sub>. A phase transition from a tetragonal to a cubic structure was

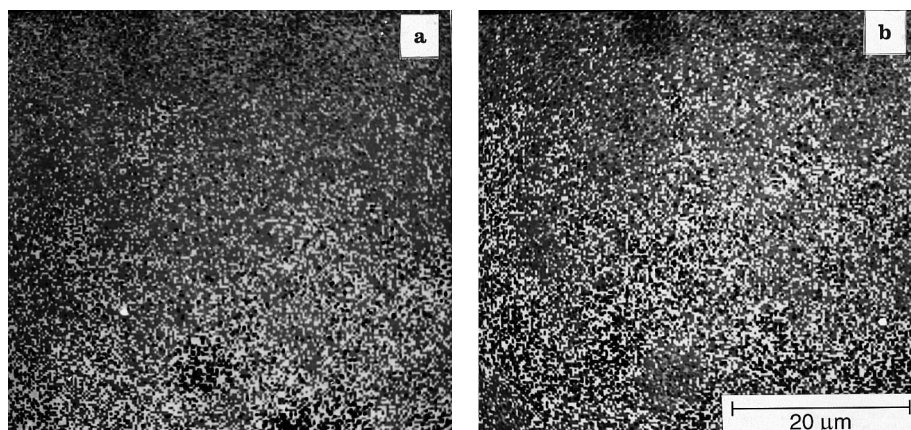


Fig. 4a, b. Surface distributions of a Pb and b Ti in the as-deposited PbTiO<sub>3</sub> thin film

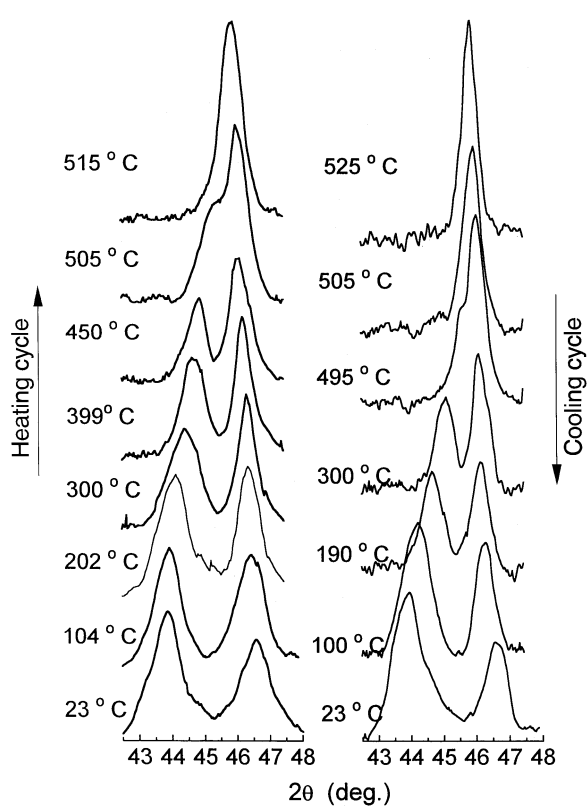


Fig. 5. Temperature dependence of x-ray diffraction profile near (002) and (200) peaks of PbTiO<sub>3</sub>

observed at about 515 °C during the heating cycle and a reverse process happened at 507 °C. This phase transition temperature upshift has been widely observed in PbTiO<sub>3</sub> thin films [5, 9, 13, 19]. Because the substrate thermal expansion coefficient is smaller than the film, film-substrate interaction may stabilize the ferroelectric phase and cause the upshift of  $T_c$ . In the phase transition process, the relative diffraction intensity of the (002) and (200) plane changed with temperature, and this reflects the

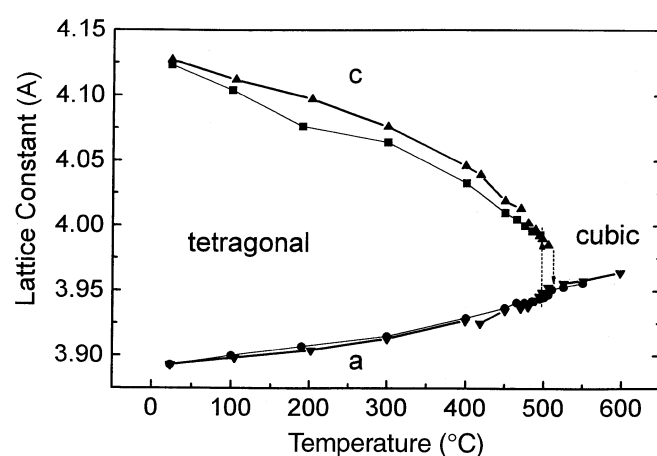
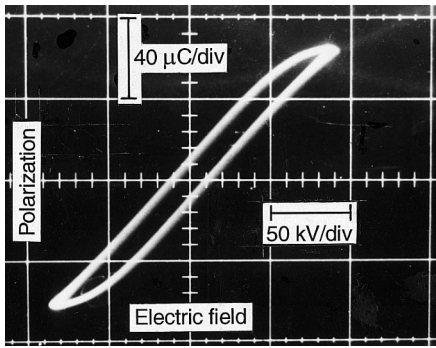


Fig. 6. The temperature dependence of the lattice constant a and c of PbTiO<sub>3</sub> thin film. Up and down triangle are the c, a lattice constants in the heating cycle, square and circle are the c, a lattice constants in the cooling cycle

domain boundary movement in the thin film. In the heating cycle, the c domains minificate while a domains enlarge. Figure 6 is a lattice parameter vs. temperature plot, the c-axis lattice constant exhibits a hysteresis in the cooling process compared to the heating process, but the a-axis length changed almost the same way on heating and cooling cycles.

The ferroelectric properties of the PbTiO<sub>3</sub> thin film were examined on a Sawyer-Tower circuit. An Ag pad with diameter of 0.7 mm was evaporated onto the surface of the heterostructure to form the top electrode, the Si substrate used as bottom electrode was contacted from the edge of the sample with Ag paint. No poling procedure was taken before the measurement. Figure 7 is a typical D-E hysteresis loop measured with a 50 Hz sinusoidal electric field. The measured remnant polarization  $P_r$ , spontaneous polarization  $P_s$  and coercitive field  $E_c$  were 10  $\mu\text{C}/\text{cm}^2$ , 52  $\mu\text{C}/\text{cm}^2$  and 11.9 kV/cm, respectively, which shows a smaller  $P_s$  and larger  $E_c$  compared to the single crystal whose  $P_s$  and  $P_r$  are 75  $\mu\text{C}/\text{cm}^2$  and 6.75 kV/cm. The decreasing of  $P_s$  seems related to the



**Fig. 7.** D-E hysteresis loop of the MOCVD  $\text{PbTiO}_3$  thin film. The measurement was taken using the redoping Si substrate as the bottom electrode

c-axis shortening from the size-induced ferroelectricity weakening.

In summary, (001) textured pure perovskite  $\text{PbTiO}_3$  thin films have been successfully deposited on Si substrates. The microstructure of low pressure MOCVD  $\text{PbTiO}_3$  thin films was investigated by AFM, EP, SEM and XRD  $\theta$ - $2\theta$  scan. A higher phase transition temperature has been found for the film compared to single crystal materials. Ferroelectric properties of the film were measured using the redoping Si single crystal substrate as the bottom electrode, indicating the possibility of make ferroelectric devices directly on the Si substrate.

*Acknowledgements.* The authors would like to thank Dr. S.B. Xiong for the ferroelectric properties measurement. Financial support from the National 863 High Technology Program of People's Republic of China is acknowledged.

## References

1. Landolt-Borstein III/I6a, Springer, Berlin, 77 (1981)
2. S.L. Swartz and V.E. Wood: *Condens. Matter. News* **15**, 4 (1992)
3. J.F. Scott and C.A. Paz De Araujo: *Science* **246**, 1400 (1989)
4. R. Vest: *Ferroelectrics* **102**, 53 (1990)
5. B.S. Kwak, E.P. Boyd and A. Erbil: *Appl. Phys. Lett.* **53**, (1988) 1702
6. Y. Gao, G. Bai, K.L. Merkle, H.L.M. Chang and D.J. Lam: *Thin Solid Films* **235**, 86 (1993)
7. M. Okada, S. Takai, M. Amemiy and K. Tomanaga: *Jpn. J. Appl. Phys.* **28**, 1030 (1989)
8. B.S. Kwak, A. Erbil and B.J. Wilkens: *Phys. Rev. Lett.* **68**, 3733 (1992)
9. Y.F. Chen, T. Yu, J. X. Chen, L. Sun, P. Li and N.B. Ming: *Appl. Phys. Lett.* **66**, 148 (1995)
10. M. de Keijsers, G.J.M. Dormans, J.F.M. Cillessen, D.M. de Leeuw and H.W.H. Zandbergen: *Appl. Phys. Lett.* **58**, 2636 (1991)
11. G.R. Bai, H.L.M. Chang, C.M. Fosterr, Z. Shen, D.J. Lam: *J. Mater. Res.* **9**, 156 (1994)
12. G.J.M. Dormans, P.J. Van Veldhoven and M. de Keijsers: *J. Cryst. Growth* **123**, 537 (1992)
13. Y.F. Chen, J.X. Chen, L. Sun, T. Yu, P. Li, N.B. Ming and L.J. Shi: *J. Cryst. Growth*, **146**, 624 (1995)
14. L. Sun, Y.F. Chen, T. Yu, J.X. Chen and N.B. Ming: *J. Phys: Condens. Matter* **7**, 6537 (1995)
15. T. Nakamura, Y. Nakao, A. Kamisawa and H. Takasu: *Appl. Phys. Lett.* **65**, 1522 (1994)
16. R. Ramesh, W.K. Chan, B. Wilkens, H. Gilchrist, T. Sands, J.M. Tarascon, V.G. Keramidias, D.K. Fork, J. Lee, and A. Safari: *Appl. Phys. Lett.* **61**, 1537 (1992)
17. R. Ramesh, A. Inam, W.K. Chan, B. Wilkens, K. Myers, K. Remsching, D. L. Hart, J.M. Tarascon: *Science* **252**, 944 (1991)
18. K.M. Satyalakshmi, R.M. Mallya, K.V. Ramanathan, X.D. Wu, D.C. Gautier, N.Y. Vasanthacharya and M.S. Hende: *Appl. Phys. Lett.* **62**, 1233 (1993)
19. K. Iijima, Y. Tomita, R. Takayama, and I. Ueda: *J. Appl. Phys.* **60**, 361 (1986)